Printing thin-film transistors with a semiconductor channel based on indium–gallium–zinc oxide

© V.V. Ivanov, D.D. Kazarinova, A.A. Lizunova, I.A. Volkov, I.S. Vlasov, E.V. Kolisova, I.A. Tsaplin, D.V. Kornyushin, V.A. Voroshilova, A.A. Loshkarev

Moscow Institute of Physics and Technology (National Research University) (MIPT, Phystech), Dolgoprudny, Russia

E-mail: ivanov.vv@mipt.ru

Received March 31, 2026
Revised May 29, 2026
Accepted June 1, 2026

The influence of the electrode formation method, annealing atmosphere and route, gate dielectric thickness, and oxide semiconductor stoichiometry on the on-off current ratio (I_{on}/I_{off}) of a transistor with an indium gallium zinc oxide (IGZO) semiconductor channel is analyzed. It is found that the transistor architecture with a lower gate and an upper pair of silver drain-source electrodes, formed by dry aerosol printing, allows increasing the charge mobility to $1.4\,cm^2/(V \cdot s)$. A hybrid approach for fabricating the transistor functional layers is proposed, which involves forming the IGZO semiconductor channel by inkjet printing and silver drain-source contacts by dry aerosol printing. The developed approach ensures the production of transistors with I_{on}/I_{off} up to $1.4 \cdot 10^4$ and a charge mobility up to $0.08\,cm^2/(V \cdot s)$.

Keywords: IGZO, thin-film transistor, dry aerosol printing, inkjet printing, post-processing.

DOI: 10.61011/SC.2026.02.63747.9325

1. Introduction

Methods of printed electronics based on using functional ink are an actively developing area, providing for the direct integration of electronic components into non-volatile wearable sensors, transparent and flexible displays, flexible energy stores and sensor systems. Methods of ink jet and aerosol printing provide for the environmentally and economically effective alternative to lithography in production of modules not requiring high resolution [1], at the expense of reduction of the number of process stages, absence of high technology operations and expensive equipment, and also the ability to shape microstructures of complex geometry in flexible and 3D substrates [2,3]. Transistors are a key building block for the implementation of logical elements, memory cells, optoelectronics devices, sensor screens and energy conversion and control systems.

The progress in the field of development of a fully printed transistor is inextricably linked to the improvement of the materials for each of the key components of the structure: a semiconductor channel, current-conducting electrodes and a gate insulator, and also the technologies for formation and post-treatment of an active element with the purpose to improve the electrical characteristics of thin film transistors (TFT) with preservation of high stability and low cost of manufacturing [4,5].

One of the promising types of materials for a semiconductor channel is metal oxides that are actively used in TFT, in particular, indium–gallium–zinc oxide (IGZO). This material provides for high mobility of charge carriers up to $39.7\,cm^2/(V \cdot s)$ [6,7], has transparency in the visible range of light and may be used to fabricat a semiconductor channel of TFT by direct printing from the precursor solutions with subsequent annealing at relatively low temperatures $300-500\,^\circ C$ [4,8].

Thin IGZO films with the thickness of $10-50\,nm$ are traditionally obtained by methods of high frequency (HF) [9] and direct current magnetron sputtering [10] using a composite target made of In_2O_3, Ga_2O_3, ZnO powders with different composition [11,12], and the most common ratio of components is $In:Ga:Zn = 1:1:1$ [13]. Transistors on films produced by magnetron sputtering show the values of the ratio of on-state and off-state currents (I_{on}/I_{off}) to $8.7 \cdot 10^8$, mobility $2-28\,cm^2/(V \cdot s)$ [7,13,14], threshold voltage from 0.4 to 9 V [12,13,15,16]. Besides, the methods of plasma-reinforced atomic layer [17] and pulse laser deposition [18] for creation of amorphous IGZO coatings of nanometer and submicron thickness are being improved.

A fundamentally different approach compared to the methods of vapor phase deposition is the technologies of thin IGZO film production from liquid dispersions and true precursor solutions, which include centrifugation (spin-coating) [19–21] and printing methods [22]. The key advantages of printed methods are the affordable cost of equipment and operating expenses, the possibility to process flexible and 3D substrates, high locality of application, simplicity of modification of the functional layer composition, efficiency of new device prototyping. Besides, the printed methods provide for the possibility to fabricate the structures of complex geometry, which compare favorably to spin-coating, since they require smaller consumption of ink, which is especially important in operation with the expensive materials.

Liquid ink used is dispersions of IGZO nanoparticles or mixtures of true solutions precursors, which after special treatment form a solid IGZO layer [21]. Nanoparticles

are obtained, for example, by sol gel synthesis [23] and method of reversed micelles [24], after which the mixture is placed into a buffer solution with a stabilizing agent and subjected to ultrasonic dispersion [19,20] and sedimentation in a centrifugal field. To prepare the ink based on true solutions, the precursors used are powders of gallium acetyl acetonate ($Ga(C_5H_7O_2)_3$), zinc acetyl acetonate hydrate ($Zn(C_5H_7O_2)_2 \cdot xH_2O$) indium acetyl acetonate ($In(C_5H_7O_2)_3$), dissolved in tetrahydrofurane (THF) [21]. Besides, the mixture with the required stoichiometry is obtained by mixing dehydrated zinc acetate ($Zn(CH_3COO)22H_2O$), indium nitrate hydrate ($In(NO_3)3H_2O$) and gallium nitrate hydrate ($Ga(NO_3)3H_2O$) in 2-methoxyethanol [25]. Similarly solutions of indium (III) chloride hydrate ($InCl_3 \cdot xH_2O$), gallium (III) nitrate hydrate ($Ga(NO_3) \cdot xH_2O$), acetate zinc dihydrate ($Zn(CH_3COO)_2 \cdot 2H_2O$) and antimony chloride (III) ($SbCl_3$) or tin chloride (IV) ($SnCl_4$) in ethyl alcohol, 2-methoxyethanol and monoethanolamine [26,27].

Post-treatment of coatings based on IGZO plays one of the defining roles in the formation of their high functional properties. The modern practice uses the following methods: thermal annealing, exposure to pulse radiation of a various spectral range and plasma modification of the surface [28]. Some experimental papers studied the post-treatment of transistors on IGZO films using various heating routes. It is found that thermal treatment in the temperature range of 340−550 °C at delay of 1−3 hr in the air atmosphere (in a muffle furance or on a hot plate) makes it possible to intentionally control the electric characteristics if devices [7,28].

To study the semiconductor properties of IGZO and the possibility to use it as a semiconductor channel for TFT, the researchers shape transistors of various architecture. Several main types of TFT are known [4]: with top (top-gate) and bottom (bottom-gate) [19,20] gates, top and bottom drain and–source electrodes [29]. A substrate used is silicon plates and glass [13,15] with a gate insulator from silicon oxide [5,30,31], aluminum oxide (Al_2O_3) [13,15] and hafnium oxide [32]. Electrodes of transistors are made by methods of screen printing from silver nanoparticles [31], HF magnetron sputtering from aluminum [30], gold [20] and indium−tin oxide (ITO) [5,15,17], lithography, ink jet [33] and dry aerosol printing [34,35].

Therefore, the relevant and promising area is the studies of the conditions to produce a semiconductor channel of transistors based on IGZO by methods of printed electronics. Therefore, the objective of this paper is to develop stable inks on the basis of true solutions precursors to manufacture a semiconductor IGZO channel by spin coating and ink jet printing, and also to study the effect of the annealing conditions, transistor architecture, material and method of electrode manufacturing on the electronic characteristics of transistors.

2. Materials and methods

Ink was made from the following precursors preliminarily dissolved in dimethyl formamide (DMF, Scharlab): zinc nitrate hydrate ($Zn(NO_3)_2 \cdot xH_2O$, 30 wt%), gallium nitrate hydrate (III) ($Ga(NO_3)_3 \cdot xH_2O$, 30 wt%) and indium nitrate hydrate (III) ($In(NO_3)_3 \cdot xH_2O$, 50 wt%) by Sigma Aldrich. Solutions were taken at the ratios providing for the production of two options of the final composition: $In_{6.5}Ga_{1.5}Zn_2O_{14}$ (ink 1) [31] and $In_7Ga_{1.5}Zn_2O_{14}$ (ink 2). To create ink, the produced solution was dissolved with DMF at the ratio of 1 : 2. The surface tension of ink measured with the help of a contact angle analyzer Krüss DSA25 was 39−40 mN/m at room temperature.

The modes of IGZO semiconductor layer formation by methods of centrifugation (spin-coating) and ink jet printing were developed. Substrates used were silicon plates of *p*-type with a thermal layer of silicon oxide with thicknesses of 100 and 300 nm. The gate electrodes were made of gold (Au) by photolithography (PL) method. Two approaches were used to form drain and source electrodes. In the first variant the gold contacts providing for the channel width of 500 μm and channel length of 30, 20 and 10 μm, were formed by lithography method. Then a semiconductor IGZO layer was applied on top of Au-contacts with the bottom gate and the bottom drain–source contact (Figure 1, *a*). In the second variant the silver electrodes based on silver nanoparticles (AgNP) were formed using dry aerosol printing (DAP) method on top of the semiconductor IGZO layer. Therefore, the architecture of the bottom gate with the top drain–source contact was obtained (Figure 1, *b*). Silver electrodes were printed on a unique prototype of a dry aerosol printer designed in MIPT [34], which combines four processes: generation of silver nanoparticles in agglomerates by a pulse-periodic gas discharge method, their conversion into quasi-spherical large isolated nanoparticles under exposure to laser radiation, local deposition of nanoparticles through a nozzle using a specified design pattern and laser sintering of deposited particles on the substrate. The specified method makes it possible to form metal microstructures of complex geometry with high resolution without a mask [36–38]. In this paper the process of laser sintering of conducting drain–source paths was replaced for thermal treatment at 300 °C in order to reduce the leakage currents in the end-user device. Photographs of the prepared samples and also microstructures of the surface of Ag-electrodes and semiconductor IGZO film, obtained using scanning electron microscopy (SEM), are presented in Figure 1.

The IGZO layer was formed using additive method of ink jet printing on a commercial printer Dimatix Materials DMP-2850 and the spin-coating method in a centrifuge EZ6-S (12 000 rpm, 30 s). Prior to application of the semiconductor layer, the substrate was cleaned using acetone and annealed for 15 min at 400 °C to remove organic pollutants.

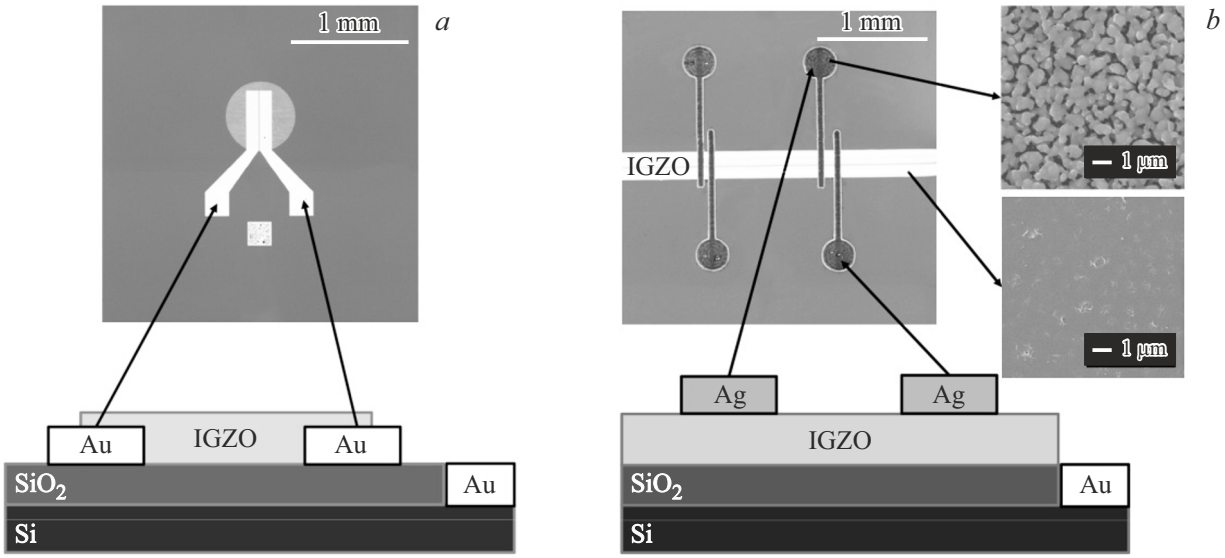

Figure 1. Circuits and microstructure of transistors with different architecture: *a* — bottom gate with bottom drain–source contact (photolithography, IGZO — spin coating); *b* — hybrid transistor with a bottom gate with a top drain–source contact (silver electrodes are formed by dry aerosol printing (DAP) method on top of the IGZO layer formed by ink jet printing), on the inserts of the SEM-image of the surface: at the bottom — IGZO film, at the top — Ag-electrode.

To obtain the complex geometry, a mask was formed on top of the centrifuged IGZO layer from polycarbonate (PC) solution in tetrachloroethane with concentration of 40−50 mg/ml. Mask layers were applied by method of microplotter printing (SonoPlot GIX Microplotter II, a glass dispenser with a diameter of 400 μm). The mask was dried at 120 °C for 1 hr, after which the samples were exposed to etching, and the semiconductor layer located under the mask preserved its properties.

Post-printing treatment of samples was annealing that was conducted in a muffle furnace (PM-1PTR) in air atmosphere, and also in a tube furnace (Rusuniversal PM-1200) in different atmospheres: mixture of argon and hydrogen (Ar+5 % H_2), nitrogen, argon and oxygen. The samples were exposed to isothermal curing at 400 °C for 1 hr. Two modes of thermal treatment were used: fast annealing — heating from 25 to 400 °C with the rate of 10 °C/min, slow annealing — two-stage heating from 25 to 80 °C for 10 min, then from 80 to 400 °C with the rate of 1 °C/min.

3. Results and discussion

The effect of atmosphere (air, O_2, N_2, Ar, Ar + 5 % H_2) and heating rate (1 and 10 °C/min) on sintering of thin IGZO films formed by spin-coating method on test structures with SiO_2-dielectric (100 and 300 nm) and Au-electrodes (channel length of 10, 20 and 30 μm). Typical transient current-voltage curves (CVC) and estimated values of charge mobility and the ratios of on-state and off-state currents I_{on}/I_{off} are presented in Figure 2, *a* and in the table, accordingly.

According to I-V data, formation of IGZO coatings in the oxygen and nitrogen atmospheres results in low semiconductor properties of transistors. Quantitatively it is expressed as limitation of the ratio of on-state and off-state currents I_{on}/I_{off} at the level of 1−3 orders, mobility μ — at the level of 10^{-4} cm^2/(V · s), which does not meet the requirements to the components of printed microelectronics. Optimal electric characteristics of transistors are achieved by annealing in a recovery atmosphere (95 % Ar + 5% H_2) with slow heating. It is important to note that thermal treatment with slow temperature rise initiates even crystallization of the IGZO film, and the average values of current ratios in the open and closed states increase 4 times relative to the fast heating route. In a series of 18 devices the average ratio of on-state and off-state currents is $I_{on}/I_{off} = 3.2 \cdot 10^4$ (maximum — $6.5 \cdot 10^4$), the mobility of charge carriers — is up to 0.02 cm^2/(V · s), and data spread is minor. When annealing in air atmosphere, similar devices demonstrate lower characteristics: values I_{on}/I_{off} in average are 3 times lower than in the samples, obtained in the mixture of argon and hydrogen. The study of the long-term stability of electrophysical parameters of field transistors after thermal annealing in air atmosphere found a heterogeneous time drift of threshold voltage in the interval from −0.3 to +3 V. At the same time the ratio of on-state and off-state currents demonstrates relative stability, being contained within one order.

To estimate the effect of the dielectric silicon oxide layer thickness, two samples of the IGZO film were made by spin-coating, on top of which DAP was used to apply silver electrodes (samples S12 and S13). According to the transfer characteristics, shown in Figure 2, *b* (dark blue and

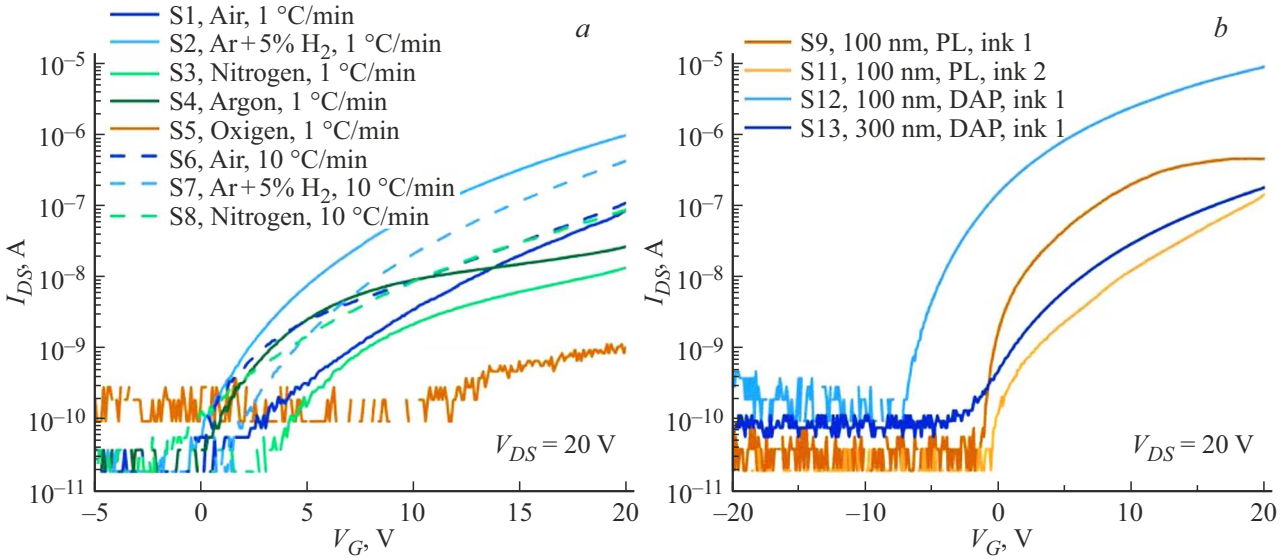

Figure 2. Current-voltage curves of transistors: *a* — effect of atmosphere and rate of annealing at transient characteristics (dependences of drain–source current I_{DS} on voltage on the gate V_G) of the IGZO samples; *b* — effect of the ink composition, thickness of the gate dielectric and transistor architecture on the transfer characteristics of IGZO samples. The coatings were obtained by spin–coating method, the measurements were made at fixed drain–source voltage $V_{DS} = 20$ V.

Architecture, post-treatment and electrophysical characteristics of produced transistors

Sample	Method of IGZO application	Electrodes	Atmosphere of annealing	Route of annealing	Thickness SiO_2, nm	I_{on}/I_{off}		μ, $cm^2/(V \cdot s)$	
						Maximum	Average	Maximum	Average
S1	Spin-coating	Au (PL)	Air	1 °C/min, 400 °C, 1 h	100	$8.5 \cdot 10^3$	$4.0 \cdot 10^3$	$2.0 \cdot 10^{-3}$	$7.6 \cdot 10^{-4}$
S2			Ar+5% H_2		100	**$6.5 \cdot 10^4$**	$3.2 \cdot 10^4$	$2.1 \cdot 10^{-2}$	$8.1 \cdot 10^{-3}$
S3			Nitrogen		100	$1.4 \cdot 10^3$	$5.8 \cdot 10^2$	$2.5 \cdot 10^{-4}$	$1.2 \cdot 10^{-4}$
S4			Argon		100	$1.7 \cdot 10^3$	$1.0 \cdot 10^3$	$5.0 \cdot 10^{-4}$	$2.1 \cdot 10^{-4}$
S5			Oxygen		100	$1.6 \cdot 10^1$	$8.1 \cdot 10^0$	$1.6 \cdot 10^{-5}$	$1.0 \cdot 10^{-5}$
S6			Air	10 °C/min, 400 °C, 1 h	100	$2.1 \cdot 10^4$	$7.1 \cdot 10^3$	$2.3 \cdot 10^{-3}$	$1.0 \cdot 10^{-3}$
S7			Ar+5% H_2		100	$5.2 \cdot 10^4$	$2.2 \cdot 10^4$	$9.5 \cdot 10^{-3}$	$4.2 \cdot 10^{-3}$
S8			Nitrogen		100	$8.1 \cdot 10^3$	$3.2 \cdot 10^3$	$2.1 \cdot 10^{-3}$	$8.2 \cdot 10^{-4}$
S9			Air	1 °C/min 400 °C, 1 h	100	$1.8 \cdot 10^4$	$5.4 \cdot 10^3$	$4.8 \cdot 10^{-3}$	$2.1 \cdot 10^{-3}$
S10			Air	1 °C/min, 350 °C, 1 h	100	$1.7 \cdot 10^4$	$5.3 \cdot 10^3$	$3.2 \cdot 10^{-3}$	$9.8 \cdot 10^{-4}$
S11 (ink 2)			Air		100	**$6.4 \cdot 10^4$**	$1.0 \cdot 10^4$	$3.4 \cdot 10^{-3}$	$1.2 \cdot 10^{-3}$
S12		Ag (DAP)	Air	1 °C/min 400 °C, 1 h	100	$2.4 \cdot 10^4$	$2.0 \cdot 10^4$	$1.4 \cdot 10^0$	$8.2 \cdot 10^{-1}$
S13			Air		300	$2.2 \cdot 10^3$	$1.3 \cdot 10^3$	$8.5 \cdot 10^{-3}$	$5.3 \cdot 10^{-3}$
S14 (ink 2)	Ink jet printing		Air	10 °C/min 400 °C, 0.5 h	100	**$1.4 \cdot 10^4$**	$4.8 \cdot 10^3$	**$8.4 \cdot 10^{-2}$**	$3.4 \cdot 10^{-2}$

light blue curves), and the estimated values of transistor amplification (see table), the reduction in the thickness of the gate dielectric allows to increase by more than 1 order the ratio of on-state and off-state currents and charge mobility in the semiconductor film.

Increase of the atomic fraction of indium within the ink with $In_{6.5}Ga_{1.5}Zn_2O_{14}$ (ink 1, S2) to $In_7Ga_{1.5}Zn_2O_{14}$ (ink 2, S11) causes a slight reduction of the average value of on-to-off currents, and the most achievable values I_{on}/I_{off} remain at the same level. It

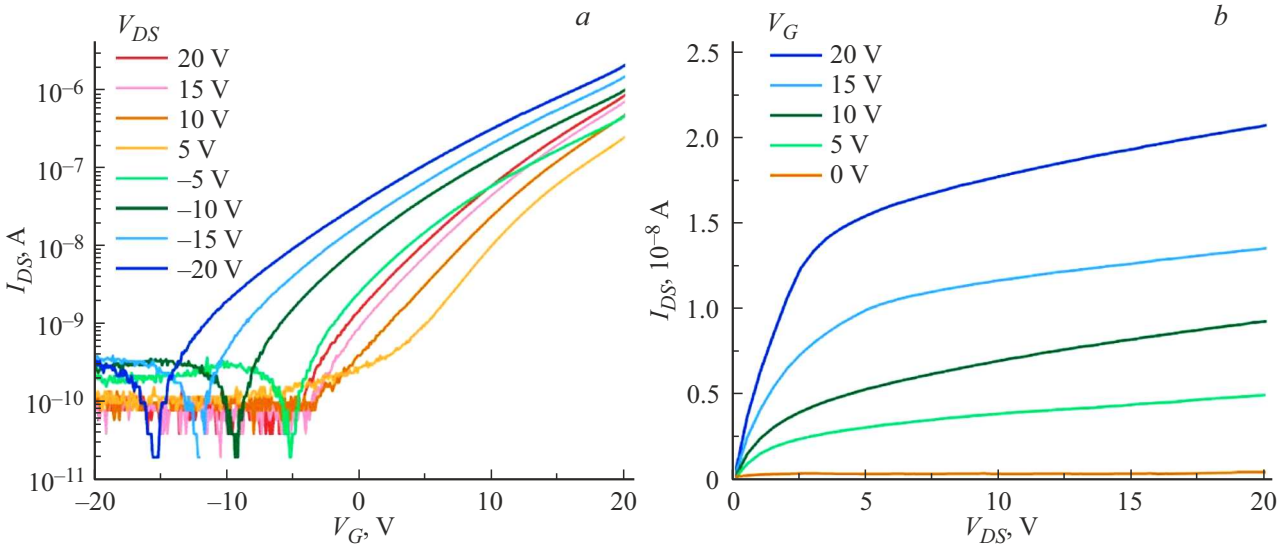

Figure 3. Series of transient (*a*) and output (*b*) characteristics of hybrid transistors with a semiconductor IGZO channel obtained by the method of ink jet printing and silver electrodes formed by dry aerosol printing.

was found that change of the ink composition requires correction of the optimal mode and annealing atmosphere. In particular, for the films with higher content of indium, the best semiconductor properties are observed after annealing on air at 350 °C. Contrary to the film with high fraction of indium, low temperature annealing of the sample with composition $In_{6.5}Ga_{1.5}Zn_2O_{14}$ in air atmosphere gives three times lower values I_{on}/I_{off} and charge mobility.

The comparative analysis of different types of transistor architecture based on S9 and S12 samples shows that in average the ratio of currents I_{on}/I_{off} is growing 4 times — to $2.4 \cdot 10^4$ in formation of the silver electrodes on top of the semiconductor layer made by the spin-coating method, and the mobility increases by 2 orders and reaches the value of $1.4\,cm^2/(V \cdot s)$ in the structure with top drain–source electrodes (Figure 1, *b*) compared to the gold contacts made by photolithography method.

Semiconductor IGZO layers formed by ink jet printing had thickness from 45 to 65 nm, the width of the line was from 150 to 246 μm. The values of the transistor channel length depended on the distance between the drain–source electrodes, which was specified according to the design pattern in the dry aerosol printer program. The real values of the channel length measured by the method of optical profilometry were from 34 to 96 μm. It was possible to achieve the maximum values of mobility at channel length of 90 μm. Specific output and transient characteristics of a hybrid transistor are shown in Figure 3.

Transient I-Vs demonstrate the typical behavior of the transistor with the *n*-type of conductivity. It was established that the threshold closing voltage substantially depends on the selected operating voltage (drain–source voltage). The maximum absolute value of threshold voltage is observed at negative operating voltages and increases when the potential on the gate increases. In the mode of positive operating voltages the threshold voltage decreases: the transistor goes into the open state at gate voltages in the range from −5 to +2 V.

Other experimental studies demonstrate high sensitivity of electrophysical characteristics of IGZO films to the parameters of temperature treatment regardless of the method of their production (magnetron sputtering and solution method) [21,39]. In particular, for the films with the composition of $In_2O_3 : Ga_2O_3 : ZnO = 1:1:1$ with thickness of 50 nm, the effect of the double-stage annealing was studied. It was shown experimentally that IGZO films exposed exclusively to single-stage annealing at 300 °C for 1 hr on air (relative humidity of 40 %) without prior thermal treatment, do not demonstrate the transient characteristics. Whereas when the annealing temperature increases at the first stage from 150 to 300 °C, non-consistent change of mobility and ratios of closing and opening currents was observed, with the maximum value of currents observed in annealing at 200 °C and was $30\,cm^2/(V \cdot s)$ and $4 \cdot 10^8$ accordingly. Additionally the directional displacement of the threshold voltage was noted from the negative to positive values with the temperature growth at the first stage.

In the studies of IGZO films with the composition of $In : Ga : Zn = 5:1:2$, produced from the mixture of nitrates [40], it was found that the increase of the annealing temperature in the range of 300–600 °C leads to the increase of the charge carrier mobility by 3 orders of magnitude — to $6.4\,cm^2/(V \cdot s)$. At the same time the threshold voltage shifts from the positive values to −37 V at 600 °C [40]. Another paper studied the effect of atmosphere at fast (1 min) annealing of thin-layer (6 and 10 nm) IGZO films, produced by a solution method from 2-methoxyethanl with the molar ratio of $In : Zn : Ga = 6:4:1$ [41]. It is shown that at 400 °C even the increase in the annealing time to 60 min does not provide for the satisfactory electrophysical

characteristics. The thickness of the film and the annealing temperature influence the optimal atmosphere of annealing, thus for 10-nanometer layers the mobility decreases in a row of He, Ar, N_2, O_2 3 times at the annealing temperature 500 °C for 1 min. The mechanism of atmosphere influence is related to the fact that high thermal speed of helium atoms ($\sim$ 3 times higher than in other gases at 500 °C) provides for better energy transfer and more effective annealing of defects, especially in the interface with aluminum electrodes.

The attempt of the researchers to design a fully printed transistor is being actively developed globally. In paper [42] a transistor is demonstrated with all layers printed on an ink jet printer, except for drain and source electrodes; and the charge carrier mobility values were achieved up to $\sim 32\,cm^2/V\cdot$ with account of the correction for the effective capacity of the device. A fully printed transistor made by ink jet printing in paper [42] included contacts from indium–tin oxide (ITO), a dielectric based on an ion gel and an active layer of IGZO with the molar ratio of In : Ga : Zn = 9 : 1 : 2. The mobility of the carriers in the active layer was $1.2\,cm^2/V\cdot s$, however, the key limitation of this technology was post-treatment — annealing at 600 °C. Such temperature is not compatible with the materials of flexible electronics (polymers, paper etc .), which substantially narrows down the area of the practical application of the device. Mobility values of 4.1 and $0.39\,cm^2/V\cdot s$, demonstrated in the studies [21,31] with $In_{6.5}Ga_{1.5}Zn_2O_{14}$ films made by spin-coating with subsequent thermal treatment at 400 °C and silver electrodes, are close to the ones presented in our paper. The method of dry aerosol printing of electrodes with low temperature annealing (200–300 °C) demonstrates high compatibility with flexible and polymer substrates providing for the required conductivity of contacts and high values of charge mobility in a semiconductor IGZO layer compared to the electrodes produced by photolithography method. However, for the implementation of the fully printed transistor on a polymer basis it is critically important to improve the technologies of posttreatment of the active IGZO layer, having reduced the temperature requirements to its formation.

4. Conclusion

It was found that the post-treatment of IGZO layers applied by the method of spin-coating using ink based on the mixture of indium, gallium and zinc nitrates (at the ratio providing for the formation of the $In_{6.5}Ga_{1.5}Zn_2O_{14}$) composition, has a fundamental importance for the achievement of high electric characteristics of transistors. The method was developed experimentally for the temperature treatment of IGZO layers with slow heating in the recovery atmosphere, representing a mixture of argon and 5 % hydrogen, making it possible to achieve the following key parameters of transistors: the average value of the ratio of on-state and off-state currents I_{on}/I_{off} — $3.2\cdot 10^4$ (maximum value — $6.5\cdot 10^4$); mobility of charge carriers — $0.02\,cm^2/(V\cdot s)$, narrow range of values of I_{on}/I_{off} within one chip. For comparison: in the atmospheres of argon, nitrogen and oxygen the ratio on-off currents in average reaches $\sim 10^3$, in air atmosphere — $6\cdot 10^4$, wide range of values. It is also shown experimentally that when the thickness of the gate dielectric SiO_2 decreases from 300 to 100 nm, the average ratio of on-state and off-state currents increases practically by an order, and the mobility value grows. It is shown that the transistor architecture of the bottom gate with top drain–source silver electrodes type, produced by the dry aerosol printing method, with a semiconductor produced by spin-coating, makes it possible to increase the charge mobility by 2 orders of magnitude and to achieve the value of $1.4\,cm^2/(V\cdot s)$.

The hybrid technology of transistor manufacturing was proposed, which has a significant potential for the development of printed microelectronics. The essence of the approach consists in the combination of two methods for application of the functional layers: a semiconductor layer is formed by ink jet printing; metal electrodes of drain–source contacts are made by the method of dry aerosol printing. The use of this arrangement made it possible to produce a transistor based on ink from a mixture of nitrates providing for the composition of $In_7Ga_{1.5}Zn_2O_{14}$ with subsequent annealing in the air atmosphere at 400 °C, makes it possible to achieve values $1.4\cdot 10^4$ and $0.08\,cm^2/V\cdot s$ for the current ratios $I_{on}/I_{off}$and mobility of charge carriers, accordingly.

The produced results indicate the promising nature of the hybrid printed technology as the effective area for the improvement of the elemental base of microelectronics.

Funding

The studies were conducted with the support of the Ministry of Science and Higher Education of the Russian Federation under the agreement No. 075-15-2024-560.

Acknowledgments

The studies for the manufacture of transistor structures by photolithography and electron microscopy methods were conducted on the equipment of the MIPT Collective Use Center.

Conflict of interest

Authors declare no conflict of interest.

References

[1] C.H. Choi, L.Y. Lin, C.C. Cheng, C.H. Chang. ECS J. Solid State Sci. Technol., **4** (4), P3044 (2015). DOI: 10.1149/2.0071504jss

[2] A.S. Dahiya, D. Shakthivel, Y. Kumaresan, A. Zumeit, A. Christou, R. Dahiya. Nano Converg., **7** (1), 33 (2020). DOI: 10.1186/s40580-020-00243-6

[3] C. Hu, B. Li, X. Wang, C. Liu, D. Sun, H. Cheng. Light Sci. Appl., **14** (1), 355 (2025). DOI: 10.1038/s41377-025-01958-z
[4] F. Chen, M. Zhang, Y. Wan, X. Xu, M. Wong, H.S. Kwok. J. Semicond., **44** (9), 091602 (2023). DOI: 10.1088/1674-4926/44/9/091602
[5] Y.S. Kim, T. Hwang, H.J. Oh, J.S. Park, J.S. Park. Adv. Mater. Interfaces, **11** (15), 2301097 (2024). DOI: 10.1002/admi.202301097
[6] W.S. Liu, C.H. Hsu, Y. Jiang, Y.C. Lai, H.C. Kuo. Membranes, **12** (1), 49 (2021). DOI: 10.3390/membranes12010049
[7] J.S. Lee, S. Chang, S.M. Koo, S.Y. Lee. IEEE Electron Dev. Lett., **31** (3), 225 (2010). DOI: 10.1109/LED.2009.2038806
[8] J. Biggs, J. Myers, J. Kufel, E. Ozer, S. Craske, A. Sou, C. Ramsdale, K. Williamson, R. Price, S. White. Nature, **595** (7868), 532 (2021). DOI: 10.1038/s41586-021-03625-w
[9] Y. Liu, B. Sun, Y. Shu, X. Zeng, J. Zhu, J. Yi, J. He. J. Mater. Res. Technol., **9** (3), 5331 (2020). DOI: /10.1016/j.jmrt.2020.03.059
[10] D. Kim, J. Jang, S. Yoon, M. Hong. ECS Trans., **64** (10), 85 (2014). DOI: 10.1149/06410.0085ecst
[11] J. Kim, S. Lv, W. Wang, S. Zheng, C. Wang, Q. Xin, Y. Li, A. Song, J. Kim, J. Jin, J. Zhang. Front. Mater., **12**, 1 (2025). DOI: 10.3389/fmats.2025.1735405
[12] M.S. Kim, H.T. Kim, H. Yoo, D.H. Choi, J.W. Park, T.S. Kim, J.H. Lim, H.J. Kim. ACS Appl. Mater. Interfaces, **13** (27), 31816 (2021). DOI: 10.1021/acsami.1c05565
[13] N. Mohammadian, B.C. Das, L.A. Majewski. IEEE Trans. Electron Dev., **67** (4), 1625 (2020). DOI: 10.1109/TED.2020.2976634
[14] B.A. Kazarkin, A.A. Stepanov, E.V. Mukha, I.I. Zakharchenya, E.A. Khokhlov, A.G. Smirnov. Dokl. BGUIR, **7** (125), 101 (2019) (in Russian). DOI: 10.35596/1729-7648-2019-125-7-101-106
[15] X. Du, G.S. Herman. Sens. Actuators B: Chem., **268**, 123 (2018). DOI: 10.1016/j.snb.2018.04.087
[16] Y. Wang, X.W. Sun, G.K.L. Goh, H.V. Demir, H.Y. Yu. IEEE Trans. Electron Dev., **58** (2), 480 (2011). DOI: 10.1109/TED.2010.2091131
[17] T. Hong, Y.S. Kim, S.H. Choi, J.H. Lim, J.S. Park. Adv. Electron. Mater., **9** (4), 2201208 (2023). DOI: 10.1002/aelm.202201208
[18] K. Nomura, H. Ohta, K. Ueda, T. Kamiya, M. Hirano, H. Hosono. Science, **300** (5623), 1269 (2003). DOI: 10.1126/science.1083212
[19] N. Fukuda, Y. Watanabe, S. Uemura, Y. Yoshida, T. Nakamura, H. Ushijima. J. Mater. Chem. C, **2** (13), 2448 (2014). DOI: 10.1039/c3tc31944j
[20] S. Sanctis, R.C. Hoffmann, N. Koslowski, S. Foro, M. Bruns, J.J. Schneider. Chem. Asian J., **13** (24), 3912 (2018). DOI: 10.1002/asia.201801371
[21] Y. Xie, D. Wang, H.H. Fong. J. Nanomaterials, **2018** (1), 7423469 (2018). DOI: 10.1155/2018/7423469
[22] G.M. Zirnik, A.S. Chernukha, D.A. Uchaev, I.A. Solizoda, S.A. Gudkova, N.S. Nekorysnova, D.A. Vinnik. Nanosyst.: Phys. Chem. Math., **15** (4), 520 (2024). DOI: 10.17586/2220-8054-2024-15-4-520-529
[23] D.E. Zhivulin, I.A. Solizoda, G.M. Zirnik, D.A. Uchaev, A.S. Chernukha, S.A. Gudkova, D.A. Vinnik. J. Struct. Chem., **66** (7), 1360 (2025). DOI: 10.1134/S0022476625070030
[24] A. Chernukha, G. Zirnik, K. Matveev, Ya. Boleyko, T. Markin, E. Anannikov, A. Loshkarev, S. Gudkova, D. Vinnik. Zhurn. struktur. khimii, **66** (3), 142135 (2025) (in Russian). DOI: 10.26902/JSC_id142135
[25] B.Y. Su, S.Y. Chu, Y.D. Juang, S.Y. Liu. J. Alloys Compd., **580**, 10 (2013). DOI: 10.1016/j.jallcom.2013.05.077
[26] T.T. Yang, D.H. Kuo. Mater. Today Commun., **24**, 101059 (2020). DOI: 10.1016/j.mtcomm.2020.101059
[27] T.T. Yang, D.H. Kuo, K.P. Tang. J. Non-Cryst. Sol., **553**, 120503 (2021). DOI: 10.1016/j.jnoncrysol.2020.120503
[28] J. Park, Z. Xiao, S. Lv, Z. Yan, J. Zhang, J. Jin, J. Kim. Semicond. Sci. Technol., **40** (11), 115013 (2025). DOI: 10.1088/1361-6641/ae1869
[29] S.K. Park, Y.H. Kim, J.I. Han. J. Phys. D: Appl. Phys., **42** (12), 125102 (2009). DOI: 10.1088/0022-3727/42/12/125102
[30] I.S. Lee, Y.J. Tak, B.H. Kang, H. Yoo, S. Jung, H.J. Kim. ACS Appl. Mater. Interfaces, **12** (16), 19123 (2020). DOI: 10.1021/acsami.9b22831
[31] C.J. Moon, J.W. Park, Y.R. Jang, H.S. Kim. Sci. Rep., **14** (1), 1566 (2024). DOI: 10.1038/s41598-024-52096-2
[32] G. Kim, S. Kim, M. Kim, C. Choi. Appl. Surf. Sci., **689**, 162365 (2025). DOI: 10.1016/j.apsusc.2025.162365
[33] K. Liang, Y. Wang, S. Shao, M. Luo, V. Pecunia, L. Shao, J. Zhao, Z. Chen, L. Mo, Z. Cui. J. Mater. Chem. C, **7** (20), 6169 (2019). DOI: 10.1039/C8TC06596A
[34] V.V. Ivanov, V.I. Borisov, V.A. Dolgov, D.V. Kornyushin, M.S. Ivanov, V.A. Voroshilova, M.N. Urazov. Russ. J. Phys. Chem. A, **99** (12), 3114 (2025). DOI: 10.1134/S0036024425702553
[35] A. Lizunova, A. Sanatulina, A. Novoselov, E. Khramov, O. Vershinina, E. Kameneva, E. Kolisova, G. Zirnik, D. Malo, V. Ivanov. Nano-Struct. Nano-Objects, **44**, 101591 (2025). DOI: 10.1016/j.nanoso.2025.101591
[36] V. Ivanov, A. Lizunova, O. Rodionova, A. Kostrov, D. Kornyushin, A. Aybush, A. Golodyayeva, A. Efimov, V. Nadtochenko. Nanomaterials, **12** (3), 448 (2022). DOI: 10.3390/nano12030448
[37] K. Khabarov, D. Kornyushin, B. Masnaviev, D. Tuzhilin, D. Saprykin, A. Efimov, V. Ivanov. Appl. Sci., **10** (1), 246 (2019). DOI: 10.3390/app10010246
[38] A.A. Efimov, D.V. Kornyushin, A.I. Buchnev, E.I. Kameneva, A.A. Lizunova, P.V. Arsenov, A.E. Varfolomeev, N.B. Pavzderin, A.V. Nikonov, V.V. Ivanov. Appl. Sci., **11** (13), 5791 (2021). DOI: 10.3390/app11135791
[39] S. Zheng, C. Wang, S. Lv, L. Dong, Z. Li, Q. Xin, A. Song, J. Zhang, Y. Li. Nanomaterials, **15** (6), 460 (2025). DOI: 10.3390/nano15060460
[40] S. Hwang, J.H. Lee, C.H. Woo, J.Y. Lee, H.K. Cho. Thin Sol. Films, **519** (15), 5146 (2011). DOI: 10.1016/j.tsf.2011.01.074
[41] S. Kil, J. Jeong. AIP Adv., **13** (11) (2023). DOI: 10.1063/5.0174995
[42] J.R. Pradhan, M. Singh, S. Dasgupta. Adv. Electron. Mater., **8** (11), 2200528 (2022). DOI: 10.1002/aelm.202200528

Translated by M.Verenikina